Growth and Magnetic Oscillatory Exchange Coupling of Mn/Fe(001) and Fe/Mn/Fe(001)

D. A. Tulchinsky[1], J. Unguris[*], and R. J. Celotta

Electron Physics Group, National Institute of Standards and Technology, Gaithersburg, MD 20899-8412

The magnetic ordering and the interlayer exchange coupling in Mn and Fe/Mn wedge structures grown epitaxially on Fe(001) whisker substrates were investigated using scanning electron microscopy with polarization analysis (SEMPA). In bare Mn/Fe(001) samples, the magnetization of the top Mn layer is collinear with the Fe magnetization, and oscillates between ferromagnetic and antiferromagnetic alignment as the Mn thickness increases. The period of the oscillation is two layers of Mn, consistent with the growth of an antiferromagnetic Mn wedge. The bare Mn behaves very much like antiferromagnetic Cr, however the magnetic coupling in the Fe/Mn/Fe(001) sandwich structures is very different. For Mn thicknesses greater than four layers, the coupling between the top Fe layer and the Fe whisker substrate is not collinear. Between 4 to 8 layers of Mn, the direction of the top Fe in-plane magnetization lies at an angle of 60° to 80° relative to the magnetization of the Fe substrate. Beginning at the 9th Mn layer, the direction of the coupling oscillates, with a 2 layer period, between 90° - ϕ and 90° + ϕ, where ϕ is sample dependent. Values of ϕ between 10° to 30° were observed.

PACS: 75.70.-I; 75.30.Pd; 81.15.Hi; 68.55.-a; 61.16.Bg

Keywords: Exchange coupling; Fe whisker; Mn films ; SEMPA; RHEED

[1] Present address: Naval Research Laboratory, Washington, DC 20375

[*] Corresponding author. Tel.: 1-301-975-3712; fax: 1-301-926-2746
E-mail address: john.unguris@nist.gov

Introduction

Considerable attention has recently been devoted to the study of the growth, structure [1, 2, 3], and magnetism [4, 5, 6, 7, 8] of ultra-thin Mn on Fe(001) as well as Fe/Mn/Fe exchange coupled structures [9, 10, 11]. These studies are motivated by the interesting magnetic coupling phenomena observed when two ferromagnetic layers are separated by a thin, atomically well ordered spacer [12]. In particular, Fe/Cr/Fe and Fe/Mn/Fe structures are of interest, because the intermediate spacer layers, Cr or Mn, show antiferromagnetic ordering in the bulk. In the Cr system, this magnetic ordering plays an active role in mediating the exchange coupling [13]. In a bare Cr film on Fe, the magnetization of the top Cr layer continually reverses direction with each additional layer of material [14]. In Fe/Cr/Fe exchange coupled systems, layer-by-layer oscillations are observed in the sign of the Fe substrate/overlayer coupling [15]. Meaningful comparisons between theoretical models and Fe/Cr/Fe coupling experiments are possible because Fe/Cr multilayers can be fabricated on Fe whiskers with nearly the same atomic scale precision as assumed in theoretical models.

The growth of Mn is more challenging. Bulk Mn can form complex crystal structures with many atoms per unit cell, and can only be stabilized in simple bcc or fcc structures at room temperature by alloying or epitaxial growth [2]. Epitaxial growth of Mn on Fe was studied by Kim *et al* [1] who found that Mn grows on Fe(001) in a strained body centered tetragonal (bct) structure with lattice parameters: a=0.2866 nm and c=0.3228 nm for thicknesses greater than four layers of Mn (note: for bcc Fe, a=0.2866 nm). Their data also shows that the distance between Mn layers is small (about $c/2 \approx 0.13$ nm) when the film is only two or three layers thick. For bct Mn, Krüger *et al.* [16] predict that Mn should order antiferromagnetically and tight binding calculations suggest the antiferromagnetically aligned surface moments should range from 2.2 μ_B to 3.4 μ_B [17] depending on the antiferromagnetic phase and Mn surface reconstruction. The measured room temperature values of the Mn magnetic moment for a thin film on Fe range from 1.7 μ_B to 4.5 μ_B [4, 8], which is larger than the value of 0.6 μ_B to 1.9 μ_B measured for a thin film of Cr on Fe [18].

In this paper, we report on the growth of well-characterized, epitaxial Mn wedges on Fe(001) whiskers in which the thickness of the Mn film is continuously varied from 0 to 25 layers. Scanning electron microscopy with polarization analysis (SEMPA) measurements of the bare Mn wedges show that the direction of the Mn surface moment changes with each additional

Mn layer added to the film, with odd (even) layers ferromagnetically (antiferromagnetically) aligned with respect to the underlying Fe whisker's magnetization. This observed ordering of the outermost Mn is consistent with antiferromagnetically ordered Mn ferromagnetically coupled at the Mn/Fe interface. After Fe is grown on top of the Mn wedge to complete the Fe/Mn/Fe(001) sandwich, the direction of the magnetization of the top Fe layer is found to be non-collinear with respect to the underlying Fe whisker magnetization. For greater than eight layer Mn spacers, the Fe in-plane magnetization oscillates with a two layer period between 90° - ϕ and 90° + ϕ, where ϕ is sample dependent. Values of ϕ between 10° and 30° were observed. This non-collinear magnetization was observed for Mn wedges grown at temperatures ranging from 50 °C to 250 °C and hence over a variety of growth conditions. This result is unlike previous results for Fe/Mn/Fe systems [9] and is not observed in the Fe/Cr/Fe system [14].

Experiment

The experimental procedures used to investigate the Fe/Mn/Fe coupling were similar to those used in previous SEMPA measurements of the Fe/Au/Fe, Fe/Ag/Fe, and Fe/Cr/Fe systems [19, 20, 15]. The experiments were performed in an ultrahigh vacuum scanning electron microscope with a base pressure of 7×10^{-8} Pa. The magnetic structure of the films was imaged with SEMPA [21], while the structural order and chemical composition were monitored *in situ* using reflection high-energy electron diffraction (RHEED) and scanning Auger spectroscopy, respectively.

The Fe and Mn films were grown on single crystal Fe(001) whisker substrates. Iron whiskers were used since they provide nearly ideal, well characterized, flat substrates with single atomic steps ~1 μm apart [22]. Whiskers were cleaned by cycles of Ar-ion sputtering and annealing to 750°C, until Auger spectra indicated that surface contamination (mainly oxygen) was below the minimum sensitivity of the Auger detector (~0.05 layers). RHEED patterns from cleaned and annealed whiskers showed a near perfect arc of sharp diffraction spots indicating the high quality of the Fe surface [23]. The substrate temperature was measured with a thermocouple attached to the sample holder.

Manganese was thermally evaporated from a ceramic crucible with typical deposition rates near 1 layer/min. Wedge-shaped Mn spacer films were grown by moving a shutter in front of the Fe whisker during Mn deposition. The thickness of a typical wedge varied continuously

from 0 layers to 25 layers over a distance of ~1mm. Both the quality and the thickness of the Mn wedges were monitored with spatially resolved RHEED imaging.

Iron was deposited from a high purity rod by electron beam evaporation. The Fe flux was monitored and controlled by using an aperture with an integrated ion flux monitor, tied to a closed loop controller. The controller allowed for 1% flux stability over long periods of time [24]. RHEED oscillations during Fe homoepitaxy were used to calibrate the flux controller. The growth rates for Fe were also typically about 1 layer/min.

Mn growth

Optimal conditions for Mn/Fe(001) growth were determined by evaporating Mn onto a Fe(001) whisker surface held at a constant temperature while simultaneously measuring the intensity of the RHEED specular diffraction peak as a function of deposition time. Examples of RHEED intensity oscillations are shown in Fig. 1 for depositions at 33 ± 2 °C, 100 ± 5 °C, 150 ± 6 °C, 200 ± 7 °C, and 250 ± 8 °C [25]. All these growths from show strong initial RHEED oscillations for the first two to three layers, which then decay in intensity at a rate that depends on the growth temperature. The decay at low temperatures (<100 °C) is suggestive of kinetically roughened growth, where the roughness is due to the limited diffusion of Mn on the surface. At higher temperatures, the RHEED oscillations continue to thicker Mn films. The growth at 150°C consistently exhibited the greatest number of oscillations, routinely at least 20 layers. The 150°C growth shown in Fig. 1 has oscillations up to the 23rd layer. At 200 °C and above, the shape of the first few RHEED oscillations changes from the rounded peaks observed below 175 °C to more cusp-like peaks. In the Cr/Fe system, STM/RHEED comparison experiments indicated that cusp-like growth is one sign of a true layer-by-layer growth where large islands grow to complete a full monolayer before the next monolayer begins [22]. While the growth at elevated temperatures may seem better, Fe/Mn interdiffusion can be a problem. Walker and Hopster [5] found interdiffusion of Fe and Mn when samples were annealed above 150°C. When growing Fe on Mn, Andrieu et al. [4] reported that Mn migrated up through the Fe overlayers when a Fe/Mn/Fe system was annealed above 175°C. Given these constraints, we found our best growth conditions were for substrate temperatures between 150 °C and 200 °C.

Further insight into the nature of the Mn growth comes from preliminary STM/RHEED studies of the Mn/Fe system. STM images suggest that Mn grown at ~160 °C grows in a nearly layer-by-layer like manner, exhibiting a definite structural change in the Mn growth between the 2^{nd} and 4^{th} layers [26]. Such a structural change may change the electron diffraction conditions and lead to a sudden drop in the intensity of the RHEED oscillations, as was observed in this study and by Purcell *et al* [9] near these film thicknesses.

At all growth temperatures the RHEED diffraction patterns eventually loose intensity and disappear, indicating a change from a nearly layer by layer growth to rougher growth. At elevated temperatures this transition can be rather abrupt. A SEM image of a 200 °C wedge between the 14^{th} to 18^{th} layers is shown in the inset to Fig. 1. This picture shows the dramatic roughening of the growth associated with the abrupt drop in RHEED intensity. This behavior is suggestive of a Stranski-Krastanov growth mode, in which the first 10-15 layers grow nearly layer by layer before a transition to 3-dimensional growth occurs [27]. At temperatures away from the 150 °C – 200 °C good growth conditions, the transition to rough growth, indicated by the sudden drop in the RHEED spot intensity, occurs for thinner Mn films.

Magnetization measurements

Following the growth of the Mn wedge, the sample was cooled to room temperature, and the wedge thickness was measured by spatially resolved, scanning RHEED. Sample defects were used to correlate the scanned RHEED images with SEMPA images acquired later. This method eliminates any errors due to variations in the deposition rate and allows us to determine the Mn thickness in the SEMPA measurements to $\pm$ 0.1 layers.

The surface magnetization direction of the Mn wedge was then measured by SEMPA. SEMPA directly measures the magnetization of the outermost 1 nm of the sample. Two orthogonal magnetization components and the topography are imaged simultaneously and independently. In the SEMPA images we present in this paper, the component of the magnetization along the direction of the Fe whisker axis is labeled M_x while M_y is the orthogonal, in plane magnetization component. The direction of the magnetization vector is $\theta = \tan^{-1}(M_y / M_x)$. Magnetization that is collinear with the Fe substrate magnetization is primarily visible in the M_x image where white (black) domains correspond to the components of the magnetization pointed to the left, i.e., $\theta = 180°$ (right, i.e., $\theta = 0°$). Non-collinear alignment

between the top film and the substrate is visible in the M_y image, where white (black) domains correspond to magnetization in the up, i.e., $\theta = +90°$ (down, i.e., $\theta = -90°$) direction.

A SEMPA image of the M_x magnetization from an uncoated Mn wedge, grown at 150 °C, is shown in Fig 2a. The dominant feature in this image is the contrast arising from the two domains in the underlying Fe whisker. At remanence the Fe substrate has a domain wall running the length of the whisker. The opposite domains provide a useful reference check of the zero of the magnetization, i.e., the Fe whisker magnetization on one side of the domain wall is equal and opposite to that on the other side of the wall. The magnetization signal from the substrate decays with increasing Mn coverage. Superimposed on the decaying Fe contrast are weak thickness dependent oscillations arising from the reversals in the Mn surface magnetization. Other Mn wedges grown between 50 °C and 250 °C show similar magnetization oscillations.

Line scans showing the Mn thickness dependence of the measured M_x and M_y magnetization, for this Mn wedge are shown in Fig. 2b. The initial M_x magnetization from the bare Fe substrate at the beginning of the Mn wedge decreases rapidly with Mn coverage until the magnetization is determined solely by the Mn overlayers. The absence of a M_y magnetization component has two possible explanations: The simplest, and we believe most likely, is that the direction of the magnetization of the bare Mn wedge is solely parallel or antiparallel to the magnetization of the underlying Fe substrate. Alternatively, non-collinear may be present in the form of equal numbers of small domains of opposite helicity. If these domains are smaller than the SEMPA resolution (100 nm for these measurements), then the non-collinear component would average to zero and the SEMPA measurements would only observe a reduced net magnetization.

To see the Mn magnetization oscillations more clearly, a decaying exponential was subtracted from the M_x component; the result is shown in Fig. 2c. Note that simply subtracting an exponential is not the best way to extract the Mn polarization signal, especially at low Mn coverages where it could significantly underestimate the Mn polarization. A more correct approach, however, requires additional unknown information or assumptions about the Fe and Mn surface moments, Fe and Mn secondary electron yields, and growth details.

Beginning at the fifth layer, oscillations in the magnetization of the top Mn layer with a period of two layers are observed in the Mn wedge grown at 150 °C. (At 250 °C the oscillations

begin at the 3rd layer.) These oscillations are consistent with layer-by-layer thickness dependent reversals in the orientation of the magnetization of the top Mn layer, implying that these Mn layers form (001) ferromagnetic sheets that align antiferromagnetically. Walker and Hopster [5] observed similar 2 layer oscillations in the Mn magnetization at thicknesses greater than five layers of Mn using spin-polarized electron energy loss spectroscopy (SPEELS). Similar oscillations were also observed by SEMPA for Cr wedges [14]. Figure 2c also shows that the surface magnetization for odd numbered Mn layers is parallel with the substrate. Assuming the Mn is antiferromagnetically ordered inside the wedge, the observed ordering of the Mn surface moment is consistent with ferromagnetic coupling at the Mn/Fe interface, as was previously suggested by Bouarab *et a*l. [17].

In addition to the magnetization oscillations with a two layer period that occur after three Mn layers, additional magnetization changes were also observed in the first couple Mn layers. Several shallow Mn wedges were grown in order to examine the magnetization of the first few layers more closely. Figure 2d shows a line scan of the M_x magnetization component (after Fe background subtraction) from a four layer wedge grown at 175 °C. A pronounced dip in the magnetization occurs at a Mn coverage of about 0.8 layers. A second, smaller dip is occasionally observed at about 1.5 Mn layers. It is difficult to quantify these magnetization changes, however, since that would require detailed information about the Mn film structure and a more sophisticated Fe background subtraction model than the simple subtraction of an exponential. However, these fluctuations are consistently observed in Mn wedges grown across a wide range of temperatures (50 °C to 250 °C).

The origin of this magnetic fine structure is not well understood, but these observations are consistent with calculations by Wu and Freeman [28, 29]. Their model predicts that a Mn submonolayer aligns antiferromagnetically with respect to the Fe, but the full first Mn layer orders as an in-plane antiferromagnet. For subsequent layers, the ordering becomes ferromagnetic in-plane with antiferromagnetic ordering between the layers. Rader *et al.* [6] and Dresselhaus *et al.* [8], using X-ray magnetic circular dichroism (XMCD) and Roth *et al.* [7] using spin resolved core level photoemission (SR-XPS) also found evidence for antiferromagnetic coupling within the first full Mn layer. Andrieu et al [4] found using XMCD that a single layer of Mn is ferromagnetic and aligns parallel to the Fe substrate. Note that none of these other experiments used single crystal Fe whisker substrates. Instead, the Fe films were

grown on various substrate materials, suggesting that some of the discrepancies between the experiments may be related to the different film structures grown on different substrates. Our measurements suggest that the magnetic orientation of the first few layers of Mn is highly sensitive to the exact structure of the Mn grown, which, in turn, is depends on the quality and crystallographic nature of the underlying Fe.

After the magnetization orientation of the bare Mn wedge was measured, Fe was evaporated onto the wedge at room temperature and the magnetization of the top Fe layer was measured with SEMPA. Magnetization images from five Fe/Mn/Fe wedge sandwich structures grown at temperatures ranging from 50 °C – 250 °C are shown in Fig. 3. Despite the wide range of growth temperatures, different Fe whisker substrates, and different growth conditions, the SEMPA images all show the same general features. There are common intrinsic features related to the nature of the exchange coupling between the Fe layers, as well as sample dependent extrinsic features like the specific domain configurations, which are related to the local magnetostatic conditions. The intrinsic features are best seen in the M_x images, while the M_y images highlight the various domain structures.

Several general observations can be made about the exchange coupling observed in the SEMPA images in Fig. 3. For the first three Mn layers the magnetization of the top Fe layer points in the same direction as the underlying Fe whisker magnetization. Thus, for three or fewer Mn layers, direct or indirect collinear ferromagnetic exchange coupling dominates. For a Mn spacer film thicker than four layers the magnetization is no longer collinear. SEMPA images indicate that most of the magnetization is in the $\pm M_y$ direction, with a small weaker component in the $\pm M_x$ direction. Between the 5^{th} and 8^{th} Mn layers the coupling direction is somewhat sample dependent, but for more than eight layers all the wedges show some oscillating coupling with a period of two Mn layers.

Interpreting the Fe film domain images and quantifying the coupling direction is somewhat confusing because of the various redundant domain structures that are present. First, there are two equivalent sets of domains resulting from the two domains present in the Fe whisker substrate. For purposes of this discussion, we consider only one of the Fe whisker domains, the top half one in the images, so that $\theta = 0°$ (180°) is considered ferromagnetically (antiferromagnetically) aligned with respect to the underlying Fe whisker magnetization. Second, when the coupling is non-collinear, two domain orientations with equal exchange coupling

energies are possible, i. e., the exchange coupling energy at θ is the same as at -θ. Which direction is favored by a particular domain or set of domains depends on minimizing other energy contributions, such as magnetostatic and anisotropy. This degeneracy occasionally leads to a complex domain structure, especially for the thicker part of the Mn wedge, which we will discuss later.

The intrinsic thickness dependence of the coupling angle is demonstrated in Fig. 4, where line scans of the magnetization angle, θ, for Mn grown at 150 °C and 250 °C in Fig. 3 are shown. For simplicity, the line scans were taken from regions of the sample that did not have the complex domain structure. These line scans clearly show the ferromagnetic alignment of the Fe overlayer for the first four layers, and the oscillatory non-collinear alignment for greater than eight layers. The oscillations are approximately symmetric about θ = 90°, oscillating between 90° - ϕ for odd Mn layers and 90° + ϕ for even Mn layer thicknesses. Spacers consisting of odd (even) numbers of Mn layers are therefore somewhat biased toward ferromagnetic (antiferromagnetic) alignment with the Fe substrate. The amplitude of the oscillations was sensitive to sample preparation. Values of ϕ between 10° and 30° were observed for different samples and different growth conditions.

The influence of the quality of the Mn growth on the exchange coupling is clearly seen in the SEMPA images in Fig. 3. The coupling oscillations are most clearly visible for the higher temperature, 150 °C to 250 °C growths, and are barely occur in the more disordered 50 °C growth. For the higher temperatures, the oscillations disappear at the thickest Mn coverages near the onset of very rough, three-dimensional growth.

Another major difference between the different growths in Fig. 3 is the domain structure, best seen in the M_y images [30]. The degeneracy between the +θ and –θ coupling orientations sometimes leads to complex domain patterns that are different for different Fe whisker substrates and different sputter/anneal/growth cycles. We speculate that the small differences in wedge structure lead to differences in the local magnetostatic energy, which, in turn, determines the domain structure.

Higher magnification pictures of the fine-scale domain structures from the wedge grown at 250 °C are shown in Fig. 5. The magnetization directions for the different possible domain

orientations are shown schematically by the arrows in the enlarged M_y image in Fig. 5. For clarity, these arrows are tilted by more than the actual magnetization, which only oscillates between ± 8° for this particular wedge. The domains have a minimum length scales of about one μm. The details of how these microdomains form is not known. Note, however, that the domain length scales and patterns are similar to the surface step densities observed with the STM for similar whiskers [22], suggesting that the substrate roughness plays a significant role in the domain formation.

The evolution of the interlayer exchange coupling, measured as Fe was deposited on top of the Mn wedge, is shown in Fig. 6. This figure displays a series of SEMPA images from the same Mn wedge, grown at 175 °C, with varying thickness top Fe films. Magnetic contrast in the top Fe film began to appear after depositing four layers, but only ferromagnetic coupling was visible and only up to the first four layers of Mn. As more Fe was added, the coupling through the thicker parts of the Mn spacer appeared. Coupling through the 17^{th} layer of Mn was only evident after more than 16 layers of Fe were grown on top of the Mn wedge. This amount of Fe needed to see the magnetic coupling was about a factor of two larger than the amount required in earlier measurements using Cr, Ag, or Au wedges on Fe whiskers. In the Mn/Fe case, more Fe may be required because the Fe film/Mn wedge interface is rougher and the Fe needs to be thicker before it becomes sufficiently continuous to become ferromagnetic. This would also explain why the magnetization in the thicker, rougher part of the wedge requires the most Fe to become visible. An alternate possibility is that the lack of intralayer coupling in the thinnest Fe films allows the formation of very small domains that follow all of the Mn surface magnetization fluctuations. These domains would be smaller than the SEMPA resolution and not visible. In any case, once the domains became visible, they did not change significantly with increased Fe coverage. The only significant change was that the transitions between domains became more abrupt, consistent with an increase in the magnetocrystalline anisotropy for the thicker Fe film.

Discussion

Our exchange coupling results are similar to those of Purcell *et al.* [9] who used the longitudinal magneto-optic Kerr effect *ex situ* to measure hysteresis loops on epitaxially grown Fe/Mn/Fe(001) whisker samples grown at 50 °C. At thicknesses greater than seven layers, they also observed exchange coupling oscillations with a 2 layer period for up to ~15 layers of Mn.

However, no non-collinear alignment was reported and the measured coupling strength was much less than they had measured for Fe/Cr/Fe. Non-collinear coupling was observed in the magneto-optic measurements of Yan *et al.* [11]. They observed a two layer period in the coupling strength and 90° coupling, but no thickness dependent oscillations in the coupling angle at remanence. Krebs et al [31, 32] used in-plane ferromagnetic resonance to study the CoFe/Mn/CoFe system and only observed non-collinear coupling. They observed oscillatory coupling with a roughly estimated period of 4 to 5 layers of Mn, which they noted also depended on the thickness of the Mn interlayer. Non-collinear alignment was also observed by Monchesky, et al [10] when they added Mn layers to Cr spacer films in Fe/Cr/Fe(001) whisker structures.

The Fe/Mn/Fe(001) coupling is significantly different from what is seen in Fe/Cr/Fe(001) wedges where the coupling between the Fe layers oscillates between ferromagnetic and antiferromagnetic with a nearly two layer period [15]. In Fe/Cr/Fe(001) non-collinear alignment is only observed at the transitions between the ferromagnetic and antiferromagnetic alignment. At these particular thicknesses, the average bilinear coupling is very small and the biquadratic coupling dominates. In addition, the direction of the magnetization of the top Fe layer is opposite to the direction of the Cr layer on top of which the Fe is deposited. For Mn the top Fe magnetization, although primarily non-collinear, is canted in the same direction as the magnetization of the top Mn layer. This observation along with our measurements of the bare Mn and Cr wedges is consistent with ferromagnetic coupling at the Fe/Mn interface and antiferromagnetic coupling for Fe/Cr.

Our observations indicate that non-collinear coupling plays an important role in the Fe/Mn/Fe system. Slonczewski [33] has suggested several models for non-collinear coupling which are based on thickness variations in the Mn film. Rough Mn growth exposes different antiferromagnetic sublattices to the Fe layers. Depending upon the length scale of the roughness and the relative strengths of the intra- and interlayer coupling, a frustration in the alignment of the ferromagnetic Fe moments can occur. This frustration can lead to a lower energy state involving non-collinear coupling between the Fe layers. In order to differentiate between the various coupling models it is crucial to have quantitative information about the atomic scale roughness of the Mn interlayer. Future STM studies would be very useful for resolving the origin of the non-collinear magnetic coupling, if they could provide this detailed information about the growth of Mn on Fe.

In summary, we have grown high quality, epitaxial Mn layers on Fe(001) whiskers and using RHEED have found 2-dimensional growth across a wide temperature range; however, the Mn most nearly ideal growth occurs when the Fe substrate is between 150 °C and– 200 °C. SEMPA images of the uncovered Mn wedge reveal a top Mn layer magnetization that is collinear with the Fe substrate magnetization and oscillates between ferromagnetic and antiferromagnetic alignment with a two layer period. The oscillations are consistent with the growth of antiferromagnetic Mn that is aligned ferromagnetically with the Fe interface. When covered with Fe, SEMPA shows that the magnetic alignment between the top Fe film and the Fe substrate is non-collinear (i.e., at neither 0, or 180°). In addition, for Mn thicknesses greater than 8 layers, the magnetization of the top Fe overlayer oscillates with a two layer between being tilted slightly toward ferromagnetic (antiferromagnetic) alignment for odd (even) numbers of Mn spacer layers. This oscillatory non-collinear coupling appears to be unique to the Fe/Mn/Fe(001) system.

The authors thank D. T. Pierce and M. D. Stiles for stimulating discussions. This work was partially supported by the Office of Naval Research and by the National Research Council Postdoctoral Research Associateship Program.

References

1 S. K. Kim, Y. Tian, M. Montesano, F. Jona, P. M. Marcus, Phys. Rev. B **54**, 5081 (1996).

2 R. Pfandzelter, T. Igel, H. Winter, Surf. Sci. **389**, 317 (1997).

3 B. Heinrich, A. S. Arrott, C. Liu, and S. T. Purcell, J. Vac. Sci. Technol. A **5**, 1935 (1987).

4 S. Andrieu, M. Fanazzi, Ph. Bauer, H. Fischer, P. Lefevre, A. Traverse, K. Hricovini, G. Krill, M. Piecuch, Phys. Rev. **B** 57, 1985 (1998).

5 T. G. Walker and H. Hopster, Phys. Reb. B **48**, 3563 (1993).

6 O. Rader, W. Gudat, D. Schmitz, C. Carbone, W. Eberhardt, Phys. Rev. B **56**, 5053 (1997).

7 Ch. Roth, Th. Kleeman, F. U. Hillebrecht, E. Kisker, Phys. Rev. B **52**, 15691 (1995).

8 J. Dresselhaus, D. Spanke, F. U. Hillebrecht, E. Kisker, G. van der Laan, J. B Goedkoop, N. B. Brookes, Phys. Rev. B **56**, 5461 (1997).

9 S. T. Purcell, M. T. Johnson, N. W. E. McGee, R. Coehoorn, and W. Hoving, Phys. Rev. B **45**, 13064 (1992).

10 T. Monchesky, B. Heinrich, J. F. Cochran, and M. Klaua, J. Magn. Magn. Mat. **198-199**, 421 (1999).

11 Shi-shen Yan, R. Schreiber, F.Voges, C. Osthöver, and P. Grünberg, Phys. Rev. B **59**, R11641 (1999).

12 D. T. Pierce, J. Unguris, R. J. Celotta, in *Ultrathin Magnetic Structures II*, eds. B. Heinrich and J. A. C. Bland (Springer Verlag, Berlin, 1994).

13 D.T. Pierce, J. Unguris, R.J. Celotta, and M.D. Stiles, J. Magn. Magn. Mat. **200**

14 J. Unguris, R. J. Celotta, D. T. Pierce, Phys. Rev. Lett. **69**, 1125 (1992).

15 J. Unguris, R. J. Celotta, D. T. Pierce, Phys. Rev. Lett. **67**, 140 (1991).

16 P. Krüger, O. Elmouhssine, C. Demangeat, and J. C. Parlebas, Phys. Rev. B **54**, 6393 (1996).

17 S. Bouarab, H. Nait-laziz, M. A. Khan, C. Demangeat, H. Dreyssé, M Benakki, Phys. Rev. B **52**, 10127 (1995)

18 P. Fuchs, V. N. Petrov, K. Totland, M. Landolt, Phys. Rev. B **54**, 9304 (1996).

19 J. Unguris, R.J. Celotta, and D.T. Pierce,J. Appl. Phys. **75**, 6437 (1994).

20 J. Unguris, R.J. Celotta, and D.T. Pierce, J. Magn. Magn. Mat. **127**, 205 (1993)

21 M. R. Scheinfein, J. Unguris, M. H. Kelley, D. T. Pierce, and R. J. Celotta, Rev. Sci. Instrum. **61**, 2501 (1990).

22 J. A. Stroscio, D. T. Pierce, J. Unguris, R. J. Celotta, J. Vac. Sci. Technol. B **12**, 1789 (1994).

23 A. S. Arrot, B. Heinrich, and S. T. Purcell, in *Kinetics of Ordering and Growth at Surfaces*, ed. M. G. Lagally (Plenum, New York, 1990).

24 A. Band and J. A. Stroscio, Rev. Sci. Inst. **67**, 2366 (1996).

25 Error estimate corresponds to the total estimated error (1 standard deviation) including both systematic and statistical errors.

26 A. Davies, J. A. Stroscio, D. T. Pierce, and R. J. Celotta, to be published.

27 R. Kern, G. LeLay, and J. J. Metois, in *Current Topics in Materials Science*, ed. Kaldis, vol 3, chapt 3, (Amsterdam: North-Holland, 1979).

28 R. Wu and A. J. Freeman, Phys. Rev. B **51**, 17131 (1995).

29 R. Wu and A. J. Freeman, J. Magn. Magn. Mat. **161**, 89 (1996).

30 In the 50 °C, 100 °C, and 200 °C samples, a small 90° diagonal stripe domain is present in the underlying Fe whisker in addition to the usual 0° and 180° domains. The exchange coupling is unchanged by the presence of this domain. The domain merely switches the magnetization between M_y and M_x.

31 M. E. Filipkowski, J. J. Krebs, G. A. Prinz, C. J. Gutierrez, Phys. Rev. Lett. **75**, 1847 (1995).

32 J. J. Krebs, G. A. Prinz, M. E. Fillipkowski, C. J. Gutierrez, J. Appl. Phys. **79**, 4525 (1996).

33 J. C. Slonczewski, J. Magn. Magn. Mat. **150**, 13 (1995).

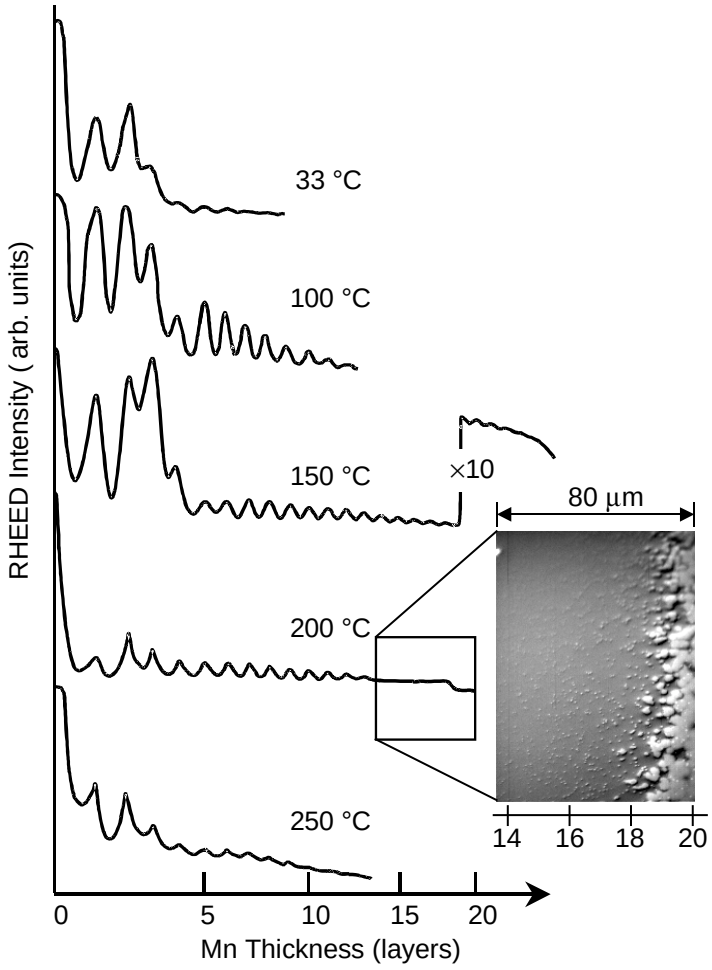

Fig 1. RHEED (0,0) beam intensity oscillations measured during the growth of Mn films on Fe(001) at 33 °C, 100 °C, 150 °C, 200 °C, and 250 °C. Oscillations were observed up to 8, 12, 23, 14, and 12 layers of Mn, respectively. The peaks in the oscillations correspond to completed Mn layers and were used to convert the abscissa's from time to Mn layer thickness. The Mn thickness scale is non-linear due to variations in the Mn flux rates during evaporation. The inset shows a topographic SEM image of the end of a wedge between the 14^{th} and 20^{th} layer of Mn grown at 200 °C showing a smooth to rough growth transition.

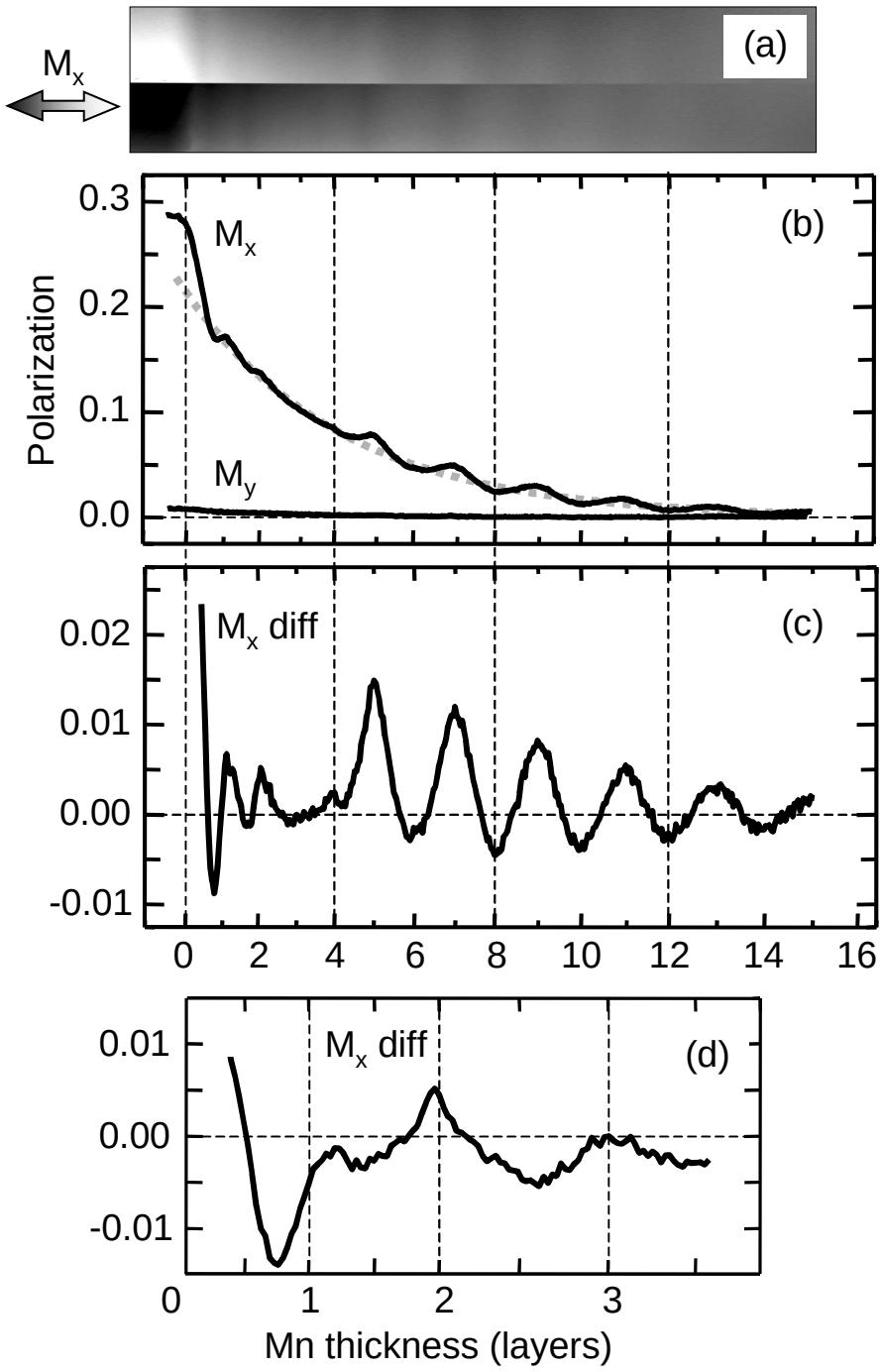

Fig 2. a) SEMPA image of the magnetization (M_x) of a bare Mn wedge grown on a Fe(001) single crystal whisker substrate at 150 °C. b) Line scans in both the M_y and M_x directions of the magnetization of the Mn wedge. The dashed line is the exponentially decaying Fe background magnetization used to calculate the data for 2c. c) Data from the M_x line scan of 2b after subtracting the exponential background. d) SEMPA line scans of the first three layers of a shallow Mn wedge grown at 175 °C showing the M_x component of the magnetization. The Fe background magnetization has been subtracted from this data as in 2c.

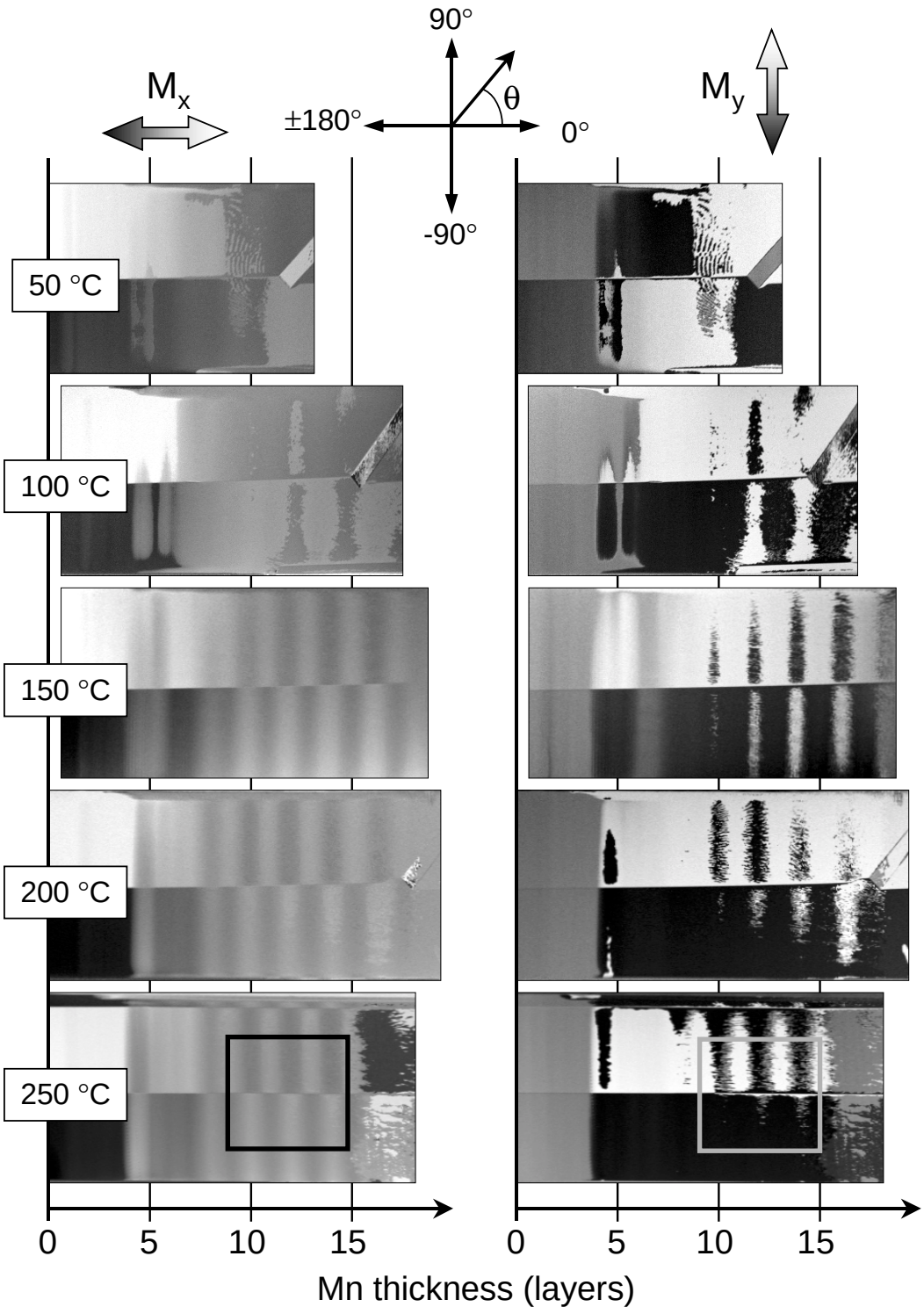

Fig 3. M_x and M_y components of the magnetization vs. Mn thickness for Mn wedges grown at 50 °C, 100 °C, 150 °C, 200 °C, and 250 °C.

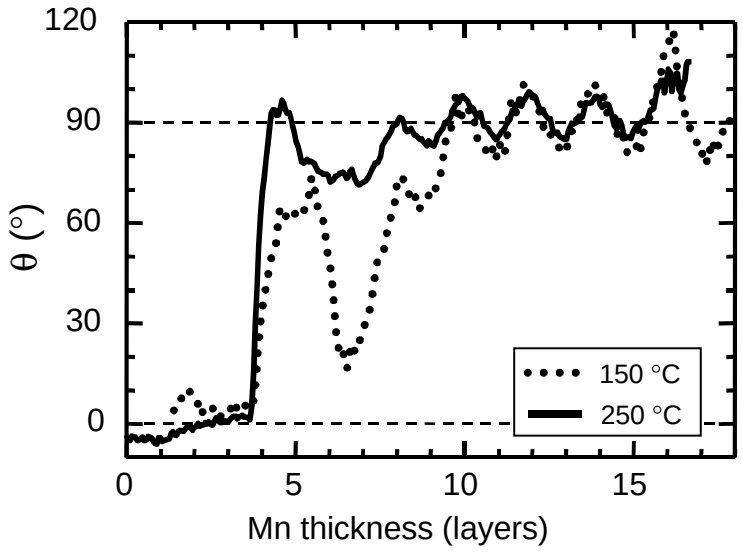

Fig 4. Line scans of the magnetization direction from the 150 °C and 250 °C SEMPA data in from Fig. 3. The line scans were taken from single domain regions avoiding complications due to the complex, degenerate domain structure.

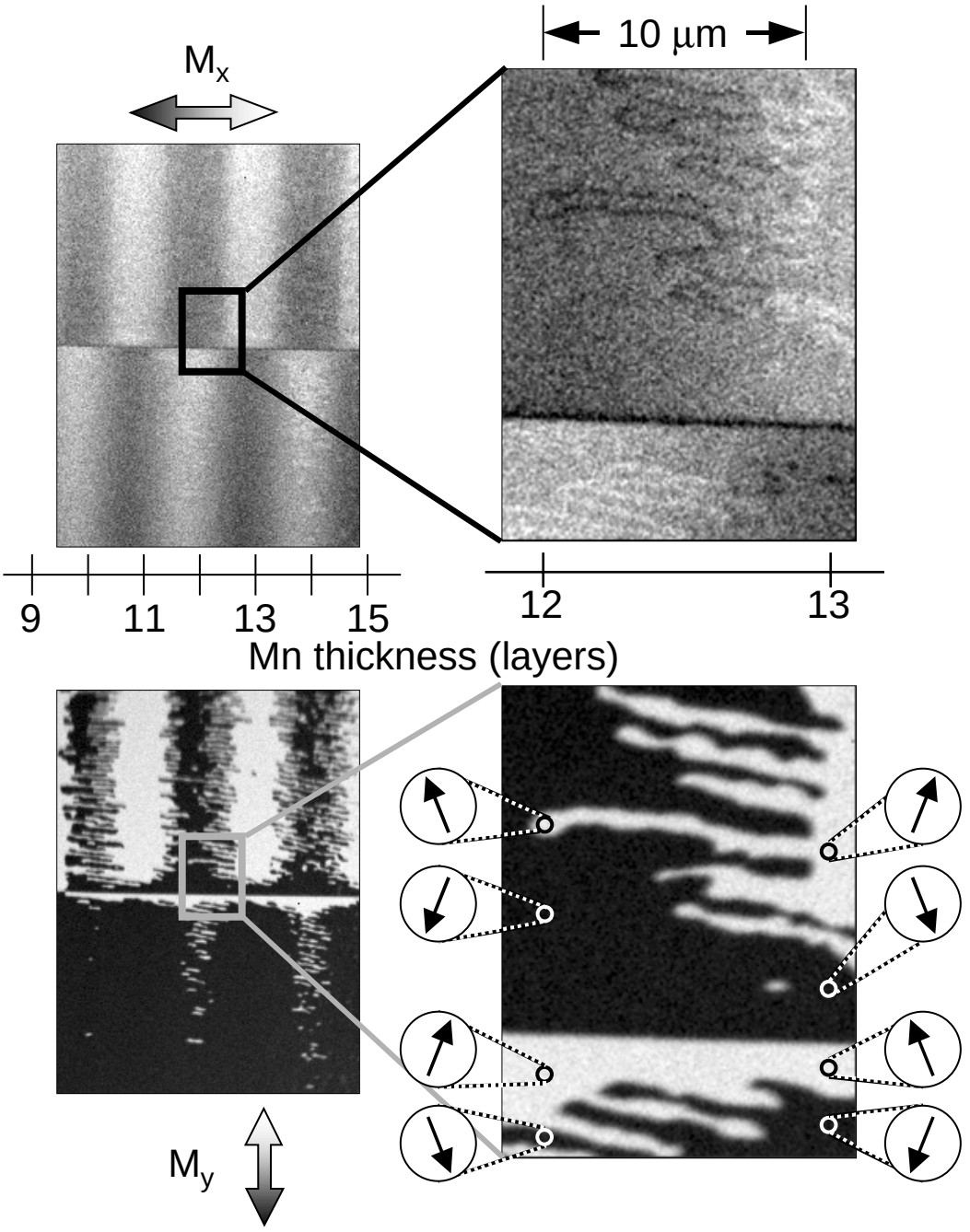

Fig 5. High resolution SEMPA images of the M_x and M_y magnetization components from the thick end of the Mn wedge grown at 250 °C. The lower magnification image is from the boxed region in the 250 °C image in Fig. 3. Eight possible domain orientations for the 12^{th} and 13^{th} layers are represented schematically by the circled arrows.

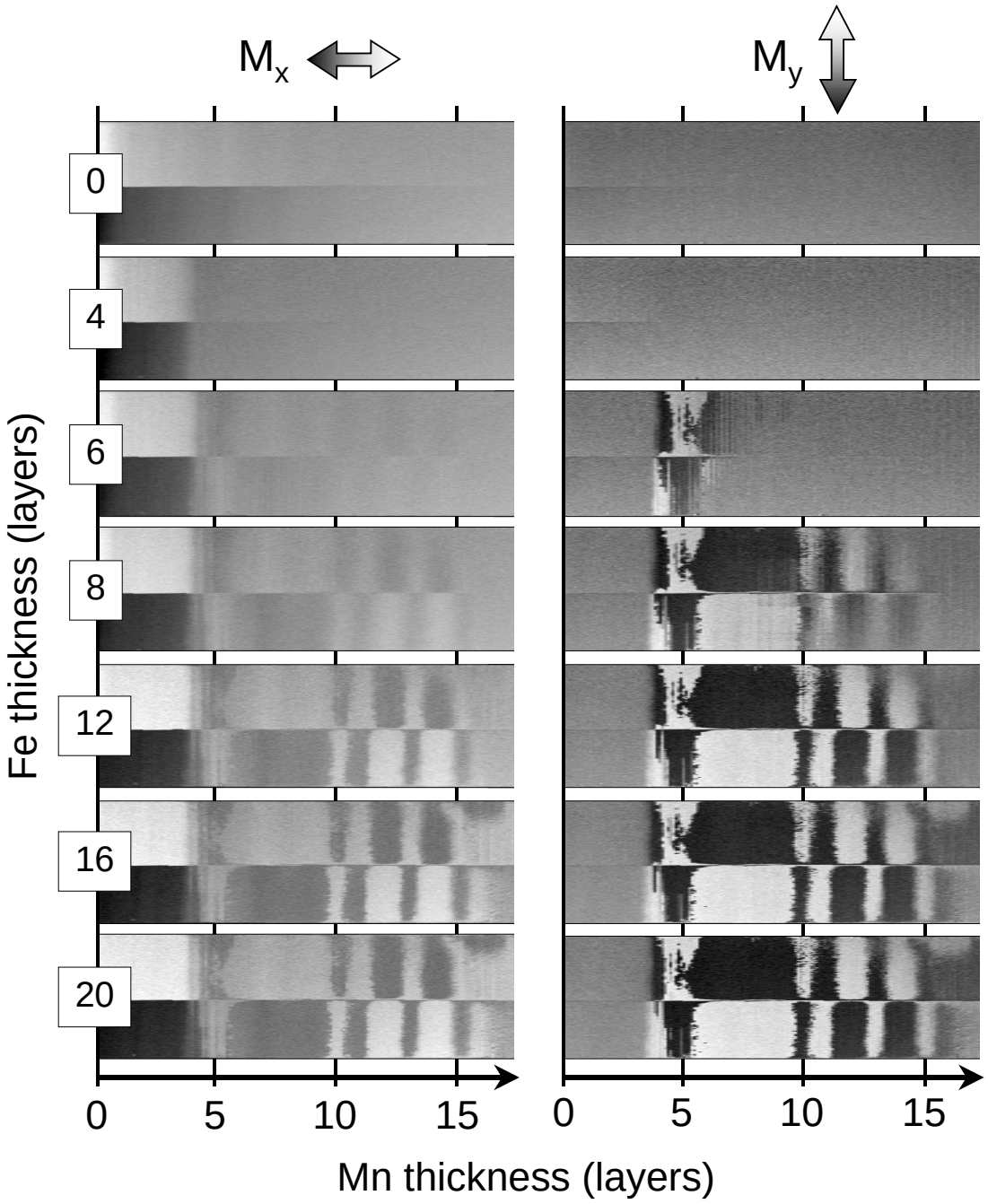

Fig 6. M_x and M_y components of the magnetization from a Mn wedge grown at 175 °C for Fe overlayer thicknesses of 0, 4, 6, 8, 12, 16, and 20 layers. Exactly the same gray scale was used for each image to facilitate comparison.